4.6. Implanted Gases on Atmosphereless Celestial Bodies

L. V. Starukhina

The interest for solar wind implanted gases is due to the prospect of extraction of potential thermonuclear fuel ^{3}He, as well as to the fact that implanted hydrogen can be ascribed to water in different types of remote sensing experiments.

Implanted hydrogen in lunar regolith

The surfaces of airless celestial bodies are exposed to energetic protons – mainly to solar wind protons of keV range. They provide severe radiation damage in the rims of

regolith particles creating trapping sites for the implanted solar wind ions. In silicates, important case of trapping sites are broken chemical bonds of oxygen atoms; they tend to be saturated by the implanted H-atoms so that OH-bonds are formed [e.g., Zeller et al. JGR. 1966. 71. 4855]. Irradiation-induced OH-groups were found by optical absorption near 3 μm, which is due to O-H stretch of hydroxyl groups. Thus, the implanted protons can be detected by optical spectroscopy near 3 μm and be mistaken for OH groups in water molecules.

Our estimates of the upper limit of concentration of solar wind hydrogen trapped per unit area of rims of lunar regolith particles, in particular, in OH groups, yield $n_s \approx (1 \div 5) \times 10^{17}$ cm^{-2}. This is in agreement with laboratory experiments. Mass fraction of the implanted hydrogen [H] = $Sm_p n_s$ for typical specific surface area of regolith S = 800 - 5000 cm^2/g (m_p is proton mass) is at least 130 ppm, but even the maximum [H] = 1700 ppm found in neutron spectrometry experiment on Lunar Prospector [Feldman et al. JGR. 2001. 106. 23,231] can be achieved at moderate values of $n_s = 2 \times 10^{17}$ cm^{-2}. If this hydrogen is interpreted as a constituent of water ice, its weight fraction can be up to a few wt.%. Thus, the excess hydrogen found on the Moon can be of solar wind origin and not belong to water molecules.

Optical effects of solar-wind-induced OH

A 3-μm absorption band was observed in reflectance spectra of asteroids of different taxonomic classes, including E and M types supposed to be differentiated and hence dehydrated. This unexpected absorption can be due to OH-groups of solar wind origin. We simulated this effect on the base of our model of spectral albedo of multicomponent regolith-like surface. The model enabled us to calculate the change in reflectance of featureless continuum when rims of regolith particles contains OH-groups. Simulated 3-μm bands are presented in Fig. 30. It shows that, if the variance of spectral positions of OH absorption maxima near different cations is taken into account, neither depth nor width, shape and position of 3-μm band can be used to distinguish between H_2O molecules or true hydrosilicates and OH-groups of radiation origin, at least at low band depths (which is the case for most observations). In Fig. 31 calculated 3-μm depths of irradiation origin are compared with those observed for asteroids, OH-concentration taken about the upper limit. Fig. 31 shows that only 3-μm bands of Pallas, Ceres, and Virginia are deeper than it could be due to solar wind OH, and thus can be interpreted as due to hydrosilicates. Calculations of band depths due to 1wt.% water ice (Fig. 31) show

that fine ice particles can contribute to 3-μm absorption much stronger than solar wind OH, and the contribution of coarse ice particles would be negligible.

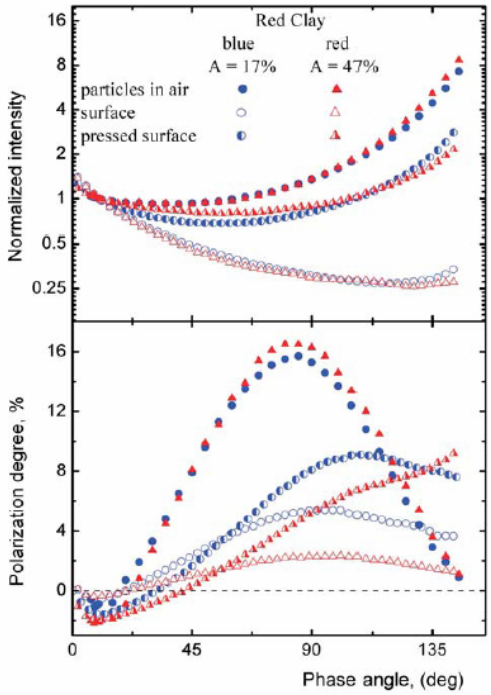

Figure 28. Photometric and polarimetric phase curves for particulate surfaces (compressed and uncompressed) and aerosol particles measured at λ=0.44 and 0.63 μm for the red clay powder. The intensity is normalized to unity at the phase angle 10°

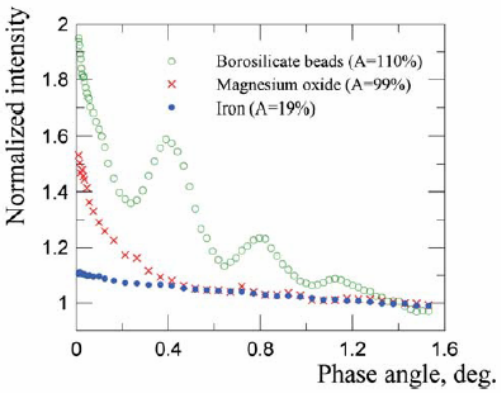

Figure 29. Normalized photometric phase curves of 3 samples measured at λ= 0.63 μm. The normalizing angle is 1.5°

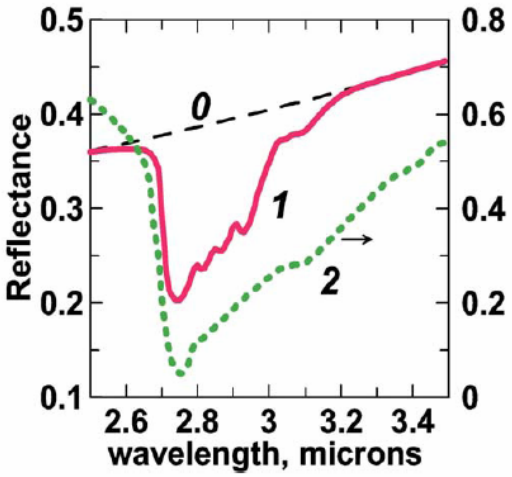

Figure 30. Simulation of effects of hydroxyl of solar wind origin (*1*) on a featureless spectrum (*0*). For comparison, 3-m band of montmorillonite (*2*) is shown (its scale is on the right)

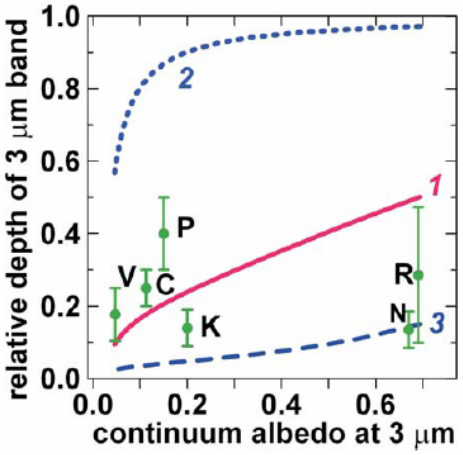

Figure 31. Calculated normalized depths for the solar-wind-induced 3 μm bands of complicated shapes (*1*) and for 1 wt.% of fine (*2*) and coarse (*3*) ice particles vs. surface albedo. Points present the deepest 3 μm band depths for asteroids: Virginia (V), Ceres (C), Pallas (P), Roxane (R), Kalliope (K), and Nysa (N)

Distribution of solar wind implanted gases: the effect of temperature and material

The implantation origin of the hydrogen detected on the Moon by Lunar Prospector is supported by the observed regional variations of the excess hydrogen. They are of two

types: (1) global, temperature-correlated, excess H being concentrated in the polar regions; (2) local spots of excess H in equatorial regions and lack of H in some permanently shaded areas. The local variations cannot be explained by ice hypothesis; both types of variations are consistent with the implantation hypothesis.

Saturation of a particle on the lunar surface with H-atoms takes ~10^2–10^3 years, which is much shorter than solar wind exposure of the particles, so even polar regions are saturated with the implanted hydrogen, the Earth magnetosphere being the source of protons for permanently shaded areas. Therefore, H-abundance is controlled by degassing processes. Their rate is extremely sensitive to temperature: ~exp(–U/kT). At low temperature, the implanted atoms become “frozen” into the regolith particles, which provides global [H] trend. Variations of trapping energies U with mineral type as well as thermal and irradiation history can provide selective gas accumulation or degassing and irregular local features: high U are responsible for excess H in “hot” regions and low U can account for lack of H in cold areas.

A similar global and local distribution can be expected for the other solar-wind-implanted elements, e.g., for ^{3}He. Thus, polar regions of the Moon are the most promising place to extract this potential thermonuclear fuel.